Available online at www.sciencedirect.com

ScienceDirect

Scripta Materialia 71 (2014) 29–32

Scripta MATERIALIA

www.elsevier.com/locate/scriptamat

Unravelling the structural and chemical features influencing deformation-induced martensitic transformations in steels

G.K. Tirumalasetty,[a,b,*] M.A. van Huis,[b,c] C. Kwakernaak,[d] J. Sietsma,[d] W.G. Sloof[d] and H.W. Zandbergen[b,*]

[a] *Materials innovation institute (M2i), Mekelweg 2, 2628 CD Delft, The Netherlands*

[b] *Kavli Institute of Nanoscience, Delft University of Technology, Lorentzweg 1, 2628 CJ Delft, The Netherlands*

[c] *Soft Condensed Matter, Debye Institute for Nanomaterials Science, Utrecht University, Princetonplein 5, 3584 CC Utrecht, The Netherlands*

[d] *Department of Materials Science and Engineering, Delft University of Technology, Mekelweg 2, 2628 CD Delft, The Netherlands*

Received 25 August 2013; revised 27 September 2013; accepted 28 September 2013
Available online 3 October 2013

A combination of electron backscattered diffraction and high-sensitivity electron probe microanalysis was used to correlate the changes in microstructural features upon deformation with local chemical composition in transformation-induced plasticity steels. A novel cleaning procedure was developed that allows complete monitoring of transformation and deformation processes in relation to the local crystal structure, microstructure and chemical composition. Here we show direct evidence that local variations in manganese content enable a gradual transformation of the retained austenite grains.

Keywords: Transformation-induced plasticity (TRIP) steel; Electron backscattered diffraction (EBSD); Electron probe microanalysis (EPMA); Chemical mapping; Martensitic transformation

The intriguing phenomenon of martensitic (diffusionless) phase transformations occurring during deformation was recognized by Sauveur [1] in 1924 by means of his torsion tests on iron bars. Surprisingly, it led to a substantial increase in ductility, and the effect was later termed transformation-induced plasticity (TRIP) [2]. The first practical exploitation of the TRIP effect came in 1967 from Zackay and co-workers, who developed steels with dramatically improved elongation as a consequence of the deformation-induced martensitic transformation [3]. Considerable scientific and technological interest grew in the early 1970s in the field of zirconia-containing ceramics exhibiting such phase transformations [4]. The concept of deformation-induced phase transformation has also been applied to polymers [5] and brittle bulk metallic glasses [6], and very recently to titanium-based biomedical alloys [7]. In view of the technological importance, there is a strong interest in understanding deformation-induced phase transformations, in particular to assess the role of various microstructural parameters such as the local chemical composition [8], grain size [9], crystal lattice orientation in relation to strain direction [10] and the location of the grain in relation to its surrounding grains [11]. An accurate understanding of all these factors and their interplay will allow fine tuning of phase transformations resulting in an enhanced control over the material properties [12].

Despite the fact that steels are amongst the most extensively investigated materials, many features of the martensitic transformation process during deformation remain unclarified to date. In particular, the role of alloying elements such as C, Mn, Si and Al during transformations is poorly understood [13] and there is an increasing need to gain fundamental insights into this topic. In this study, two steels, with chemical compositions of (wt.%) Fe−1.65Mn−1.53Si −0.037Al−0.199C (Si-alloyed TRIP steel) [11] and Fe−1.62Mn−0.35Si−0.91Al−0.187C (Al-alloyed TRIP steel) [14], are investigated. Both of these steels are commercially produced on an industrial

* Corresponding authors at: Kavli Institute of Nanoscience, Delft University of Technology, Lorentzweg 1, 2628 CJ Delft, The Netherlands. Tel.: +31 15 2781536; fax: +31 15 2786600 (G.K. Tirumalasetty); e-mail: ganeshkumar.india@gmail.com

1359-6462/$ - see front matter
http://dx.doi.org/10.1016/j.scriptamat.2013.09.027

hot dip galvanizing line using a conventional intercritical annealing cycle followed by cooling to around 400–460 °C, isothermal holding at this temperature and finally cooling to room temperature.

In order to obtain combined information of the crystallographic structure, orientation and chemical composition of each grain in relation to its neighbouring grains, and their changes upon an overall deformation and the strain direction, we have used a combination of two techniques: electron backscattered diffraction (EBSD) and electron probe microanalysis (EPMA). EBSD enables to monitor the microstructural changes of individual grains during deformation. For instance, we recently reported an EBSD study showing that metastable austenite grains rotate within the matrix (of ferrite) during the tensile tests in TRIP steels [11], thereby contributing to the high ductility of these steels. EPMA is a very reliable analytical technique to measure the chemical composition. Although EBSD and EPMA can provide the required information, their actual application for monitoring phase transformations is hampered by an inevitable formation of carbon contamination on the surface. This carbon layer is deposited during the measurements due to the decomposition of residual hydrocarbon gases [15] by the electron beam, which deteriorates the quality of the EBSD data and makes the EPMA carbon content analysis totally unreliable.

It is thus essential to remove the contamination formed during each EBSD and EPMA measurement prior to additional EBSD or EPMA experiments performed after straining. For this purpose, we have successfully developed a two-step plasma cleaning procedure, using a very low-energy oxygen plasma followed by a hydrogen radicals plasma (details in the supporting information (SI)). The key component is the use of low-energy hydrogen radicals, which can only result in chemical processes at the surface [16], instead of the generally used physical sputtering. We obtained excellent results using first oxygen plasma cleaning for 3 min followed by hydrogen plasma cleaning for 40 min. The EBSD data after cleaning showed the same quality as the EBSD data on the virgin surface: in both cases 85% of the EBSD patterns could be indexed, whereas with the carbon contamination layer only 10% could be indexed and with oxygen plasma cleaning alone only 30% could be indexed.

A schematic of the sample and the EBSD and EMPA measurements is shown in Figure 1. Dog-bone-shaped samples were electropolished in order to have a surface layer that is not mechanically deformed. Markers were created by indentation with a Vickers indenter, and EBSD and EPMA mapping was performed between these markers. Scanning electron microscopy (SEM) images were recorded before and after EBSD measurements to track the respective locations as shown in Figure 2. The samples were plasma cleaned after each EBSD or EMPA analysis using the cleaning procedure described above. After the EBSD and EPMA measurements, the samples were deformed and EBSD maps were recorded again on the same area. The samples were only lightly strained to follow the first transformations during the deformation process. SEM–EBSD was performed using a JEOL JSM 6500F microscope operated at 20 kV, and EPMA was performed using a JEOL JXA 8900R microprobe operated at 10 kV and 50 nA beam current with a spot size of 500 nm (more experimental details in SI).

Figures 3A and S2A show a typical TRIP steel microstructure consisting of ferrite matrix (coloured green) and metastable grains of retained austenite (coloured red). Retained austenite, which has a face-centred cubic structure, and ferrite, which has a body-centred cubic structure, can be easily distinguished by EBSD software because of their different crystallographic structures. Grains of martensite, grain boundaries and areas with a high dislocation density are not indexed by the EBSD software due to the poor quality of the Kikuchi patterns and are imaged in black in the phase identification maps. An EPMA line scan was performed on the EBSD mapped regions, as shown in Figures 3A and S2A, and the corresponding elemental compositions of the retained austenite grains are plotted in Figures 3C–E and S2C–E. Among all of the austenite grains intersected by the

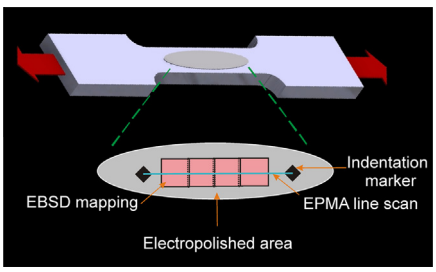

Figure 1. Schematic of a dog-bone-shaped TRIP steel sample subjected to tensile deformation. The inset shows the central electropolished area where adjacent EBSD maps and an EPMA line scan are recorded between markers. The indentation markers are also visible in the experimental SEM images (Fig. 2). Experimental details are given in the SI.

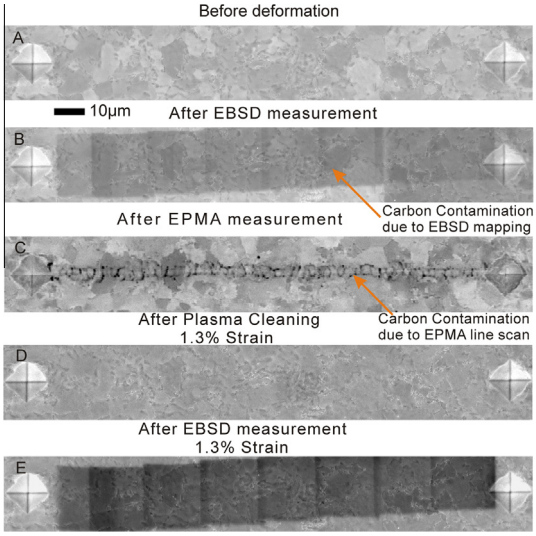

Figure 2. (A, B, D, E) SEM and (C) backscattered EPMA image of Al-alloyed TRIP steel indicating carbon contamination caused by EBSD mapping (B, E) and by the EPMA line scan (C). (D) Removal of carbon contamination by plasma cleaning.